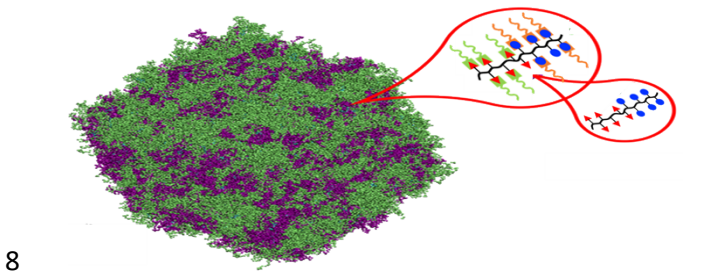
- A Modular Approach for the Synthesis of Bottlebrush Diblock Copolymers from
- 2 Poly(Glycidyl Methacrylate)-block-Poly(Vinyldimethylazlactone) Backbones
- Bin Hu¹, Jan-Michael Carrillo¹, Liam Collins¹, Kevin S. Silmore², Jong Keum¹, Peter V.
- 4 Bonnesen¹, Yangyang Wang¹, Scott Retterer¹, Rajeev Kumar^{1,*}, and Bradley S. Lokitz^{1,*}
- ¹ Center for Nanophase Materials Sciences, Oak Ridge National Laboratory, Oak Ridge, TN 37831, USA
- ² Chemical Engineering, Massachusetts Institute of Technology, Cambridge, MA 02139, USA
- 7 *Corresponding author email: <u>kumarr@ornl.gov</u>; <u>lokitzbs@ornl.gov</u>



9 For Table on Contents use only: MD Simulations of Bottlebrush Diblock Copolymers

10 Abstract

11 A strategy that enables the facile synthesis of bottlebrush block copolymers with flexible backbones was developed. A demonstration of the strategy's utility was carried out by grafting 12 13 end functionalized polymethylmethacrylate (PMMA) and polystyrene (PS) to the dually reactive block copolymer, poly(glycidyl methacrylate)-block-poly(vinyldimethylazlactone) (PGMA-b-14 15 PVDMA). Five different bottlebrush diblock copolymers were investigated by SEC, ¹H NMR, FT-16 IR, DSC, X-ray scattering methods, AFM, rheology and computational simulations using molecular dynamics (MD) and self-consistent field theory (SCFT). A relationship between the 17 glass transition temperature and the fraction of chain ends was demonstrated by DSC and 18

highlights the potential of this synthetic method to tailor polymer properties. All five samples were found to be in a disordered phase exhibiting multi-scale structures revealed by two broad peaks in small angle X-ray scattering (SAXS) that can be attributed to graft-to-graft and backbone-to-backbone density correlations using MD simulations. The SCFT-based simulations justify the observation of a disordered phase due to its stabilization by the grafts. This modular approach can be easily extended to other grafts, including responsive, conducting, and charged polymers with the prerequisite end groups. The versatility and ease of assembling these functional bottlebrushes constitutes a powerful 'toolbox' method for the rapid and scalable synthesis of novel bottlebrush block copolymers with desired properties.

Introduction

30

31

32

33

34

35

36

37

38

39

40

41

42

43

44

45

46

47

48

49

50

51

52

The ability to create new functional materials with unique structures depends on the ability to effectively manipulate matter on the nanoscale level. By harnessing van der Waals forces, electrostatic and magnetic interactions, as well as controlling phase separation within the system, individual nanostructure and polymer building blocks can be aligned in predictable and prescribed ways. Such efforts require a detailed understanding of how polymer properties such as molecular weight, composition, and topology affect assembly at interfaces. This understanding can only come from systematic synthesis of polymers that vary these parameters individually. Bottlebrush polymers, a type of branched or grafted polymer with polymeric side chains attached to a linear backbone, can be designed in a modular manner that enables the systematic variation of polymer properties, thus providing a veritable 'toolbox' for the facile synthesis of bottlebrush block copolymers.¹⁻³ Unlike linear block copolymers, high molecular weight bottlebrushes do not entangle due to the strong, excluded volume interactions between side chains.⁴⁻⁶ Blending bottlebrush copolymers enables effective surface-active additives and can be used to tailor surface properties by blending them with other homopolymers and block copolymers.⁷⁻⁸ Other potential applications include lithography, drug delivery, photonic crystals and energy storage devices. 9-13 The three established methods to prepare bottlebrush polymers are: (1) "grafting-to"; (2) "grafting-from"; and (3) "grafting-through" and all have advantages and disadvantages. 4, 14-17 Grafting-from and graftingthrough methods can result in 100 % grafting density. However, when the grafting-from method is used, accurate characterization of the molecular weight and dispersity for the grafts and resultant bottle-brush polymer is challenging. Likewise, the grafting-through method typically requires synthesis of a macromonomer. Furthermore, longer backbone degrees of polymerizations (DP) are

difficult to achieve. 18 In contrast, by utilizing the grafting-to approach, the graft polymer molecular weight can be fine-tuned and characterized before attachment, but the grafting density for the resultant bottle-brushes are typically much lower compared to the other methods.^{5, 14, 19} Bottlebrush copolymers can be made by attaching two (or more) different types of polymeric side chains, which enable the bottlebrushes to have multiple functionalities. Examples include polystyrene-poly(lactide) (PS-PLA) and polystyrene-poly(methyl methacrylate) (PS-PMMA) bottlebrush block copolymers prepared using the grafting-from approach, 20, 45 poly(hexyl isocyanate)-poly(4-phenyl butyl isocyanate) (PHIC-PBI) bottlebrush block copolymers prepared 60 using the grafting-through approach,^{21, 22} bottlebrush random copolymers and core-shell bottlebrush copolymers prepared by the grafting-to method.²³⁻²⁴ Orthogonal approaches have also been reported including the one-pot synthesis of polystyrene-polyethylene glycol (PS-PEO) bottlebrush block copolymers prepared by simultaneous grafting-from and grafting-to methods.²⁵-²⁷ To the best of our knowledge, there are a very few reports on the synthesis of bottlebrush diblock copolymers using the grafting-to method with flexible backbones.²⁸ Here, we present a straightforward route for the synthesis of bottlebrush diblock copolymers that builds on previous work with dually reactive block copolymers.²⁹ PGMA-b-PVDMA incorporates two reactive functional groups into the block copolymer using controlled radical polymerization. An extensively studied and well-defined dually reactive diblock copolymer, PGMA-b-PVDMA was 70 adopted as the backbone of the bottlebrush copolymer and two end-group functionalized polymers,

with PS-OH and PMMA-COOH utilized as polymeric side chains, as a proof of concept. 30-33

Specific conditions were found that enabled the hydroxy-terminated PS to react exclusively with

PVDMA followed by the reaction of PMMA with carboxylic acid end groups and PGMA.³⁴⁻³⁵ A

series of bottlebrush diblock copolymers, PGMA(-g-PMMA)-b-PVDMA(-g-PS), were prepared

53

54

55

56

57

58

59

61

62

63

64

65

66

67

68

69

71

72

73

74

and investigated by nuclear magnetic resonance (NMR), size exclusion chromatography (SEC), thermal gravimetric analysis (TGA), X-ray scattering, atomic force microscopy (AFM), and computational simulations. This simple synthetic route offers a wide selection of polymeric side chains and allows enables a new path for the synthesis of bottlebrush AB diblock copolymers with targeted properties via the grafting-to method.

Experimental

Materials

All reagents, including the ring opening catalyst 1,8-Diazabicyclo[5.4.0]undec-7-ene (DBU), chain-transfer agents (CTA) 2-cyano-2-propyl dodecyl trithiocarbonate (CPDT), 4-cyano-4-[(dodecylsulfanylthiocarbonyl)sulfanyl]pentanoic acid (CDPO) and 4-cyano-4-[(dodecylsulfanylthiocarbonyl)sulfanyl]pentanol (CDPA), were purchased from Sigma Aldrich and used as-received unless stated otherwise. 2-Vinyl-4,4-dimethyl azlactone (VDMA; Isochem North America, LLC) was distilled under reduced pressure. 2,2'-Azobis(2,4-dimethylvaleronitrile) (V-65) was purchased from Wako Specialty Chemicals and recrystallized from methanol before use.

Synthesis of PGMA-b-PVDMA Diblock Copolymer

PGMA₇₂-*b*-PVDMA₁₁₁ was prepared *via* a sequential two-step reversible addition fragmentation chain transfer (RAFT) polymerization process starting from the synthesis of PGMA (**Scheme 1**).²⁹ GMA (7.245 g, 5.10×10⁻² mol), CPDT (237.5 mg, 6.75×10⁻⁴ mol; GMA:CPDT = 76:1), V-65 (35.5 mg, 1.43×10⁻⁴ mol; CPDT:V-65 = 4.7:1), and DMF (10.358 g) were added into a 50 mL two-neck round-bottom flask. The solution was sparged with nitrogen for approximately 1 h. The flask was

then placed in a heated oil bath set at 50 °C and allowed to react for 20 h. The monomer conversion 98 99 was found to be 95.5% by ¹H NMR analysis. The mixture was diluted with THF (approximately 10 mL), precipitated in hexanes three times, and dried under high vacuum. SEC analysis results: 100 101 $M_{\rm n,SEC}$ = 10.6 kDa; dispersity (Đ) = 1.15. The DP was 72, as calculated from the number average 102 molecular weight determined by SEC $(M_{n.SEC})$ data and molecular weight of GMA and CPDT. The PGMA macroCTA (2.010 g, 1.90×10⁻⁴ mol), VDMA (2.607 g, 1.88×10⁻² mol), V-65 (10.3 103 mg, 4.15×10⁻⁵ mol), and DMF (7.081 g) were added into a 50 mL two-neck flask. The solution 104 was sparged with nitrogen for 1 h before the flask was placed into a 50 °C oil bath. After 20 h, the 105 106 flask was removed from the oil bath and the mixture was diluted with 10 mL THF followed by precipitation into hexanes three times. The purified diblock copolymer was dried in vacuo and 107 analyzed by SEC and ¹H NMR spectroscopy. SEC results: $M_{n,SEC} = 26.0 \text{ kDa}$, $\Theta = 1.12$. The final 108 monomer conversion was 99.3 % as calculated from the ¹H NMR spectra. The DP of the PVDMA 109 block was 111 as calculated from the $M_{n,SEC}$ of PGMA-b-PVDMA, PGMA macroCTA, and 110 molecular weight of VDMA. 111 112 A block copolymer with a higher DP was also prepared using the same procedure. For the PGMA macroCTA the GMA to CPDT ratio was 396:1 with a 5:1 initatior to CTA ratio. SEC results: 113 114 $M_{\text{n.SEC}}$ = 42.1 kDa, D = 1.35. For the block copolymer the PVDMA to macroCTA ratio was 400:1 Sec results: $M_{n,SEC} = 96.0$ kDa and D = 1.31. The DP of PGMA and PVDMA was 338 and 343, 115 respectively. 116

Scheme 1. Synthesis of PGMA-b-PVDMA, PS-OH, and PMMA-COOH by RAFT

Synthesis of PS-OH and PMMA-COOH as Grafts

For the synthesis of PS₁₆-OH (**Scheme 1**), styrene (5.220 g, 5.02×10^{-2} mol), CDPO (944.1 mg, 2.42×10^{-3} mol), AIBN (52.7 mg, 3.21×10^{-4} mol), and DMF (2.968 g) were added into a 50 mL two-necked round-bottom flask. The molar ratio of styrene:CDPO:AIBN = 21:1:0.13. The solution was sparged with nitrogen for approximately 1 h and then placed into an 80 °C oil bath for 40 h. The reaction mixture was then precipitated in methanol three times and the purified polymer was dried *in vacuo*. SEC results: $M_{n,SEC}$ = 2.1 kDa, Θ = 1.06. The DP of PS-OH was 16, as calculated from $M_{n,SEC}$ of PS-OH and the molecular weight of styrene and CDPO.

For the synthesis of PMMA₄₈-COOH (**Scheme 1**), MMA (5.218 g, 5.22×10^{-2} mol) was combined with CDPA (491.7 mg, 1.22×10^{-3} mol), AIBN (33.0 mg, 2.01×10^{-4} mol) and anisole (5.506 g) with

the molar ratio of MMA:CDPA:AIBN = 43:1:0.16. The solution was sparged with nitrogen for

approximately 1 h and then placed into a 60 °C oil bath for 20 h. The polymer was then precipitated in hexane three times and the purified polymer was dried *in vacuo*. SEC results: $M_{n,SEC} = 5.2$ kDa, D = 1.07. The DP of PMMA-COOH was 48, as calculated from $M_{n,SEC}$ of PMMA-COOH and the molecular weight of MMA and CDPO. To vary the DP of PMMA, the MMA:CDPA molar ratio was changed while keeping the CDPA:AIBN molar ratio constant; all other procedures remained the same.

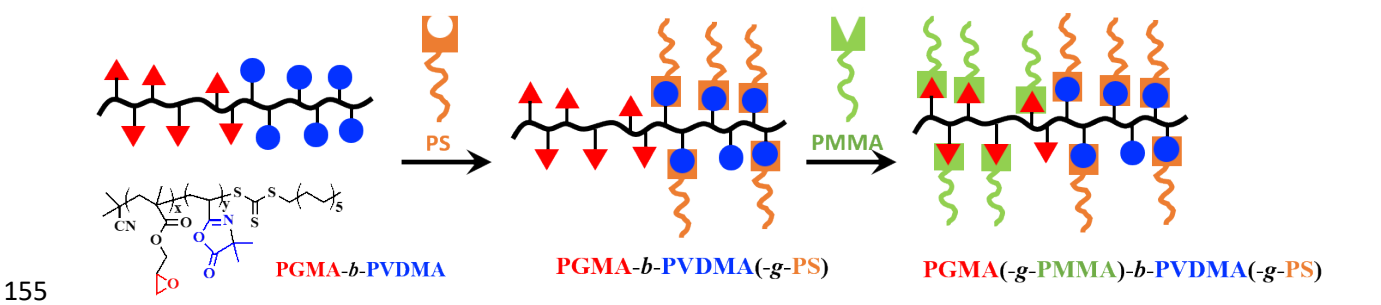
 PS_{75} -OH ($M_n = 8.2 \text{ kDa}$, D = 1.09) and PMMA₂₄-COOH ($M_n = 2.8 \text{ kDa}$, D = 1.13) were prepared using a similar method.

Synthesis of PS and PMMA-Grafted Bottlebrushes

The PGMA(-g-PMMA₄₈)-b-PVDMA(-g-PS₁₆) diblock bottlebrushes were prepared via a two-step reaction process starting from the synthesis of PGMA-b-PVDMA(-g-PS₁₆) (Scheme 2). PGMA-b-PVDMA (208.8 mg, 8.89×10⁻⁶ mol), PS₁₆-OH (1.870 g, 8.5×10⁻⁴ mol), and DMF (3.009 g) were added into a 50 mL round-bottom flask. After the polymers were dissolved by DMF, DBU (6 μ L) was injected into the solution and the flask was placed into a 35 °C oil bath for 3 days. The product was purified by dialysis (MWCO = 25,000) against acetone. SEC results: $M_{n,SEC}$ = 197.0 kDa, D = 1.33.

For the synthesis of PGMA(-g-PMMA₄₈)-b-PVDMA(-g-PS₁₆), PGMA-b-PVDMA(-g-PS₁₆) (103.5 mg, 7.60×10⁻⁷ mol), PMMA₄₈-COOH (252.1 mg, 5.36×10⁻⁵ mol), and DMF (1.078 g) were added into a 50 mL round-bottom flask. The reaction mixture was placed into a 65 °C oil bath for 2 days. The reaction mixture was then diluted with ~5 mL acetone and was transferred into a dialysis tube (MWCO = 25,000) and dialyzed against acetone to remove the excess PMMA side

chains ($M_n = 586.0 \text{ kDa}$, D = 1.49). Other PGMA(-g-PMMA)-b-PVDMA(-g-PS) bottlebrushes with different chain length of PMMA or PS were synthesized using the same procedure (**Table 2**).



Scheme 2. Synthesis of PGMA(-*g*-PMMA)-*b*-PVDMA(-*g*-PS) bottlebrushes

Characterization

 1 H NMR spectra were obtained on a Varian VNMRS 500 NMR spectrometer at room temperature in CDCl₃. Fourier transform infrared spectroscopy (FTIR) experiments were performed on a Bruker Vertex 70 with a diamond attenuated total reflection (ATR) window in the range of 4000 to 500 cm $^{-1}$. The peak resolution was set to 4 cm $^{-1}$ and each spectrum was scanned 64 times. The molecular weight of polymers and bottlebrushes were determined by SEC system using a Malvern OMNISEC equipped with a light scattering detector with a 640 nm laser and a refractive index (RI) detector with 640 nm. Three Agilent PLgel Mixed C (two columns with 5 μm particle size and 300 mm by 7.5 mm column dimensions, and one guard column with 5 μm particle size and 50 mm by 7.5 mm column dimensions) were used, and THF was the eluent with a flow rate of 1 mL/min.

°C min-1 using TA Instruments Discovery TGA. Thermal transition was measured using a TA

Instruments (TA Q2000) differential scanning calorimeter (DSC) under N₂. Reported values

171 (middle point) were from the second heating cycle of a heat/cool/heat procedure: (1) 10 °C min⁻¹

172 ramp to 350 °C, isotherm at 350 °C for 3 min, (2) 10 °C min⁻¹ quench cool to 0 °C, isotherm at 0

°C for 3 min, (3) 10 °C min⁻¹ ramp to 350 °C. The glass transition temperature (T_g) was determined

by TA Universal Analysis software.

174

175

176

177

178

179

180

181

182

183

184

185

186

187

188

189

190

191

SAXS measurements were carried out on an Anton-Paar SAXSess mc2 instrument with slit-

collimated monochromatic CuK_{α} radiation ($\lambda = 1.5406$ Å) operating at 40 kV and 50 mA. The

collimated beam size was 18 mm x 0.4 mm. The films were aligned perpendicular to the direction

of the X-ray beam (transmission mode) and the scattered beam was recorded on a CCD detector

(PI-SCX, Roper Scientific Inc.) with a pixel resolution of 2084 × 2084 and pixel dimensions of 24

× 24 μm². The slit-smeared SAXS curves were all desmeared using a desmearing algorithm

provided by Anton-Paar and expressed as intensity *versus* q, where $q = (4\pi \sin \theta)/\lambda$ after subtraction

of detector dark current and background scattering.

AFM measurements were done using a Cypher ES (Asylum Research, USA). Measurements were

performed using silicon probes AC160TS-R3, having nominal resonant frequency, $\omega_0 = 300$ kHz,

and stiffness, k = 26 N/m. Samples were mounted onto metal pucks using carbon tape prior to

taking the measurements. All measurements were carried out at room temperature (\sim 20 °C) and at

30–40% relative humidity.

Small-amplitude oscillatory shear experiments were performed on an HR2 rheometer (TA

Instruments) with 8mm-diameter parallel plates in the frequency range of 1—100 rad/s and

temperature range of 250—115°C, with a temperature increment of 5°C. The sample was

equilibrated at each temperature for 8 minutes before the frequency-sweep measurement. The

temperature control was achieved through an Environmental Test Chamber with nitrogen as the gas source.

Coarse-Grained Molecular Dynamics and Self-Consistent Field Theory Simulations

Coarse-grained molecular dynamics simulations of different bottlebrush diblock copolymer melts were performed. The chain architecture of the bottlebrush diblock copolymer consisted of N_{bb} = 32 connected backbone beads, where 16 backbone beads were grafted to sidechains consisting of A-type beads and the other half to side chains consisting of B-type beads. The degree-of-polymerization of the block A-type side chains was, N_A = 20, while that of the block B-type side chains were varied from N_B = [5, 10, 20, 40, 80].

The simulations were done in the canonical (NVT) ensemble and the constant temperature (T) was maintained by coupling the system to a Langevin thermostat as implemented in LAMMPS. $^{36-37}$ The initial configuration of the system consisted of m_b randomly oriented bottlebrush molecules arranged in a cubic n^3 lattice with lattice spacing of $2N_{bb}\sigma$, where σ is the bead diameter. The simulation box size, L (in units of σ), was gradually compressed to a final density of $0.85\sigma^{-3}$ for a simulation run of 5000τ . After compression, the system was equilibrated for an additional $20,000\tau$. Here, τ is the characteristic time defined as $\tau = \sigma(m/kT)^{1/2}$, where m is the mass of a bead and kT is the thermal energy. The production run consisted of a run, which was $80,000\tau$ long and the trajectory was sampled every 500τ resulting in 1601 trajectory frames used for the ensemble average in the calculation of scattering functions. System sizes are provided in **Table 1** and further details of the simulations are presented in the Supporting Information (SI).

Table 1. System Sizes Simulated using Molecular Dynamics Simulations.

m_b	N_{bb}	N_A	N_B	n_{total}	$L(\sigma)$
729	32	20	5	314928	71.82
729	32	20	10	373248	76.01
512	32	20	20	344064	73.97
343	32	20	40	340256	73.70
216	32	20	80	352512	74.57

 m_b : number of bottlebrush molecules, N_{bb} : Degree-of-polymerization of backbone, N_A : Degree-of-polymerization of block B side chains, n_B : Degree-of-polymerization of block B side chains, n_{total} : Total number of beads in the simulation box, n_{total} : simulation box size

To investigate the structure of the bottlebrush molecules in the melt, we calculated the partial structure factors based on the fast Fourier transform (FFT) method previously described by Carrillo et al.³⁸ The static structure factor, S(q), is defined in equation 1 as

$$S(q) = \frac{1}{n_{total}} \sum_{i=1}^{n_{total}} \sum_{k=1}^{n_{total}} f_k f_j \langle \exp(-i \vec{q} \cdot (\vec{r_k} - \vec{r_j})) \rangle$$
(1)

where $f_{i=k,j}$ is the scattering weight and is varied from either 0 or 1 depending on the type of bead, \vec{q} is the scattering vector, $\vec{r}_{i=k,j}$ is the position vector, and the bracket $\langle ... \rangle$ denotes ensemble averaging.

Large-cell self-consistent field theory (SCFT) simulations of incompressible bottlebrush diblock copolymers were also conducted using the PSim software package in two dimensions.³⁹ The bottlebrushes simulated consisted of a backbone and two different side chains (i.e., PS and PMMA) spaced equally apart and the resulting morphology of microphase separation was studied as the relative length of the side chains was varied. In the context of these simulations and the figures,

the backbone was denoted "E", the PS graft was denoted "S", and the PMMA graft was denoted "M". Other details of the SCFT based simulations and expected morphologies are presented in the SI.

231

232

233

234

235

236

237

238

239

240

241

242

243

244

245

246

247

248

249

228

229

230

Discussion

In previous work, we showed that RAFT polymerization could be used to synthesize dually reactive block copolymers containing pendant epoxy and azlactone groups.²⁹ Here, we extend that work to use PGMA-b-PVDMA block copolymers as a platform for tailored bottlebrush polymers via grafting-to reactions. A relatively low and high molecular weight polymer backbone, PGMA₇₂ $b\text{-PVDMA}_{111}$ (M_n = 26.0 kDa, Θ = 1.12) and PGMA₃₃₈- $b\text{-PVDMA}_{343}$ (M_n = 96.0 kDa, Θ = 1.31), respectively, were synthesized to investigate the versatility of the process. In addition to the SEC results, epoxy groups from PGMA were observed by ¹H NMR (assigned as peak a, b and c) and azlactone groups from PVDMA (1815 cm⁻¹) were visible by FT-IR, as shown in Figure 1, confirming that the reactive groups were available for "grafting-to" reactions. Both azlactones and epoxides are known to react with similar nucleophiles, however; previous literature reports suggested that by judicious choice of reactions conditions PGMA and PVDMA could be independently targeted. 40-41 Test reactions using small molecules with a pendant carboxylic acid and alcohol groups were used to determine the optimal reaction conditions and order to independently target either PGMA or PVDMA. A more detailed description of the test conditions can be found in Table S1. The best results were obtained when -OH groups were reacted with PVDMA using 1 mol % DBU as a catalyst at 35 °C and when -COOH groups were reacted with PGMA at 65 °C. Copolymers of PMMA and PS and their phase behavior have been the subject of numerous literature reports and were therefore chosen to serve as a model system for this process. 42-44 However, in principle any polymer with hydroxy (-OH) or carboxylic acid (-COOH) end groups could be "grafted-to" the PGMA-b-PVDMA backbone, making this platform incredibly versatile and tailorable. PMMA-COOH and PS-OH polymers were synthesized using either CDPA or CDPO RAFT agents to impart carboxylic acid and hydroxy groups, respectively. Molecular weight and dispersity results for all the polymers used in this study are summarized in **Table 2**.

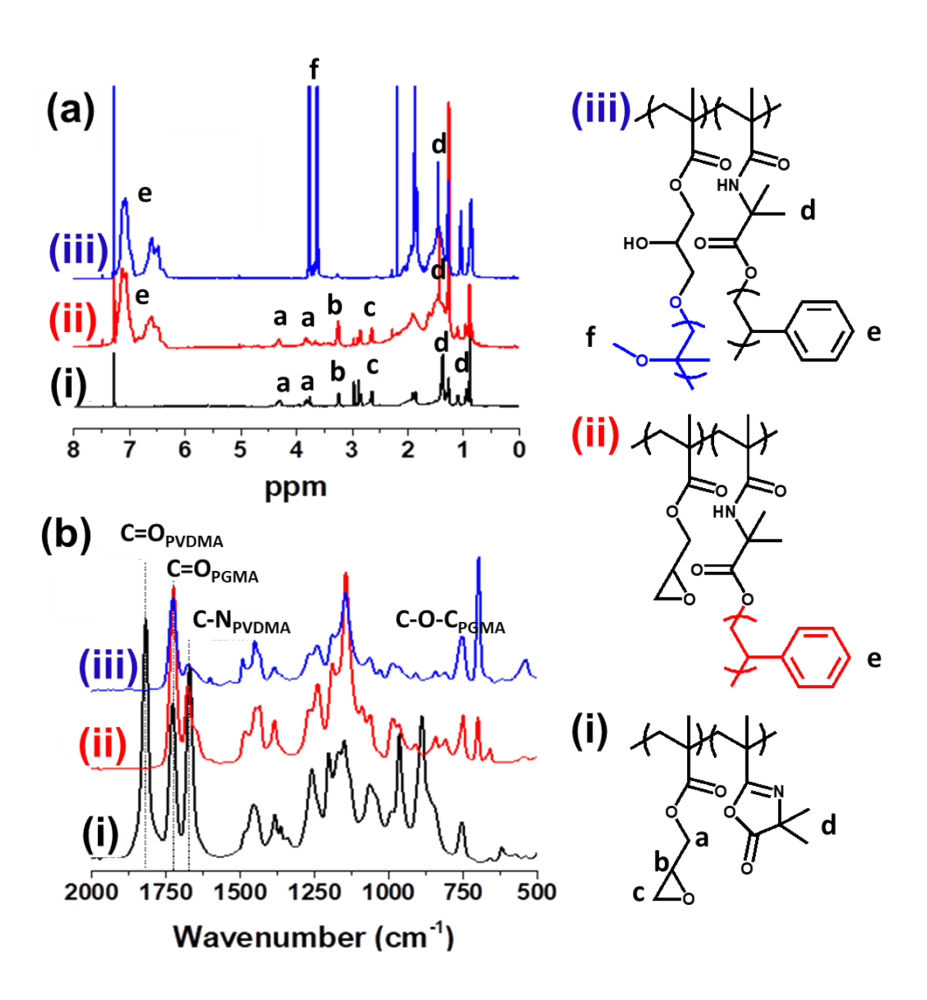


Figure 1. a)¹H NMR and b) FTIR spectra for i) PGMA₇₂-b-PVDMA₁₁₁ backbone (black), ii) PGMA-b-PVDMA(-g-PS₁₆) (red), and iii) PGMA(-g-PMMA₂₄)-b-PVDMA(-g-PS₁₆) (blue) bottlebrushes.

Table 2. Molecular weight and dispersity of PGMA-*b*-PVDMA backbones, PMMA-COOH and PS-OH.

Polymer	Molecular Weight (M _n , kDa)	Đ
PGMA ₇₂ -b-PVDMA ₁₁₁	26.0	1.12
PGMA ₃₃₈ -b-PVDMA ₃₄₃	96.0	1.31
PMMA ₂₄ -COOH	2.8	1.13
PMMA ₄₈ -COOH	5.2	1.07
PS ₁₆ -OH	2.1	1.06
PS ₇₅ -OH	8.2	1.10
PGMA ₇₂ -b-(PVDMA ₁₁₁ -g-PS ₁₆)	197	1.33
PGMA ₇₂ -b-(PVDMA ₁₁₁ -g-PS ₇₅)	719	1.31
PGMA ₃₃₈ -b-(PVDMA ₃₄₃ -g-PS ₁₆)	796	1.35

The first step of bottle-brush formation consisted of reacting the PGMA-*b*-PVDMA backbone with excess PS-OH and 1 mol% of DBU at 35°C for 3 days. The reaction was monitored by FTIR and showed the azlactone peak at 1825 cm⁻¹ decreasing in intensity while an additional peak at 1726 cm⁻¹ (**Figure 1b**) emerges and is attributed to the formation of an ester linkage between PVDMA and PS-OH. Epoxide peaks at 3.3 (CH-O-CH₂) and 2.6 ppm (CH-O-CH₂) observed by ¹H NMR (**Figure 1a - i, ii**) before and after the reaction confirm that PS-OH reacts preferentially with PVDMA. After addition of PS-OH, the epoxide peaks are still present at 3.3 and 2.6 ppm (no peak shifts) and additional peaks between 6.6 and 7.2 ppm attributed to PS aryl protons are observed.

Dialysis against acetone was used to purify the mixture; however, unreacted PS-OH could still be observed in the SEC trace but is apparently removed in subsequent reaction and purification steps (Figure S1). For the second step, PGMA-b-PVDMA(-g-PS) was reacted with excess PMMA-COOH at 65 °C. The reaction was monitored by ¹H NMR using the epoxy peaks in PGMA at 3.3 and 2.6 ppm (Figure 1a, iii). Unreacted PMMA-COOH was removed by dialysis against acetone and confirmed by SEC (Figure S1). Even though PGMA and PVDMA showed high conversions in the test reactions with small molecules, such high conversions are rare for grafting-to bottle brush systems.⁵ In total, five bottlebrush diblock copolymers were prepared by varying either the graft molecular weight or backbone length and in each case, the dispersity of the final bottlebrush broadened considerably compared to the backbone dispersity indicating a distribution of grafted polymers among the backbone chains (Table 3). For narrowly dispersed grafts such as the ones used in this work, an increase in dispersity of the bottlebrushes relative to the dispersity of the backbone is not unexpected when grafting efficiencies are less than 100%. 18 NMR was used to determine the composition of the block copolymer and the bottlebrush in order to determine the grafting density (number of side chains/number of backbone repeats) for each step. 46, 47 This was done by integrating the peaks assigned to PVDMA (1.4-1.5 ppm), PGMA (3.3 ppm), PS (6.6-7.2 ppm), and PMMA (3.6 ppm) to determine the molar composition of the block copolymer backbones and bottlebrushes and converted them to a wt %. The molecular weight of the macroCTA (PGMA), diblock (PGMA-b-PVDMA), PS-OH grafts, and PMMA-COOH grafts were all determined independently by SEC. The total molecular weight of the bottlebrushes could then be calculated using the backbone molecular weight and weight fraction determined using SEC and NMR, respectively. The grafting density of PS and PMMA for each bottlebrush is listed in **Table**

273

274

275

276

277

278

279

280

281

282

283

284

285

286

287

288

289

290

291

292

293

4 and estimated based on the total number of PS and PMMA repeat units determined from NMR (see the details of these estimations in the SI).

Table 3. Table of backbone DP, side chain composition, molecular weight, and Φ of BB-1 to BB-5.

	Backbone	PMMA	PS	Wt % PMMA	Wt % PS	MWa	Ðb
						(Da)	
BB-1	1	24	16	56.9	31.5	224,138	1.42
BB-2	1	48	16	71.1	20.0	295,454	1.49
BB-3	1	24	75	35.3	37.3	172,185	1.66
BB-4	1	48	75	32.6	45.0	116,071	1.53
BB-5	2	24	16	64.6	27.5	1,215,190	1.36

Backbone 1 stands for PGMA₇₂-b-PVDMA₁₁₁, while Backbone 2 stands for PGMA₃₃₈-b-

PVDMA₃₄₃. ^aDetermined from ¹H NMR and see the details in the SI, ^b determined from SEC.

Table 4. Table of grafting density of PS and PMMA graft of BB-1 to BB-5 determined by ¹H NMR.

	BB-1	BB-2	BB-3	BB-4	BB-5
Step 1 (PS to PVDMA)	31%	25%	7%	5%	46%
Step 2 (PMMA to PGMA)	64%	56%	31%	10%	83%

We studied the effects of chain architecture (i.e., number and length of grafts as well as backbone lengths) on the physical properties and structure of bottlebrush block copolymer melts. Many physical properties and surface segregation behavior of bottlebrushes can be attributed to having a larger number of chain ends when compared to linear polymers.^{8, 45} For instance, we probed the effects of chain ends on the T_g of bottlebrush block copolymers. In general, the chain ends are

expected to act as self-plasticizers leading to a decrease in T_g with an increase in chain end fraction compared to total monomer repeats. 46-47 The T_g of the PGMA-b-PVDMA backbones, PS and PMMA grafts, and bottlebrush block copolymers were measured by DSC, and are shown in Figure 2. PMMA-24 and PS-16 have T_g of 51.2 °C and 47.0 °C, respectively while the longer grafts, PMMA-48 and PS-75 have T_g 's of 82.6 °C and 82.2 °C, respectively. The T_g for PMMA-48 and PS-75 are slightly lower than the reported literature values, which is not unexpected since they are below the entanglement MWs for PMMA and PS. 48-49 The T_g for PGMA72-b-PVDMA111 and PGMA₃₃₈-b-PVDMA₃₄₃ are 79.0 °C and 75.7 °C, respectively (see **Table S3**). The glass transition temperature for the bottlebrush block copolymers ranged from 79.4 °C to 116.2 °C. To compare the measured changes in the T_g for the five bottlebrush block copolymers due to changes in the grafting density, graft lengths, and backbone lengths, we calculated the fraction of chain ends (f_e = n_e/DP , where n_e and DP are the number of ends and total degree of polymerization, respectively). Results from these calculations are shown in Table S4. Based on the concept of self-plasticization by the chain ends, a linear relation between $1/T_g$ and the fraction of chain ends, f_{e_i} would be expected.⁴⁶ To verify the linear relation, $1/T_g$ as a funtion of f_e was plotted in Figure 3 and a regression line with an R² value of 0.9811 confirms the relationship. What is remarkable about the data is that the similar T_g of BB-5 (96 kDa backbone) and BB-1 (26 kDa backbone) can be explained by their similar f_e values despite BB-5 being roughly five times the MW and having approximatly 5 times more chain ends than BB-1. This leads us to conclude that the chain ends act as self-plasticizers in bottlebrush block copolymers and the fraction of chain ends can be used to tailor T_g of bottlebrush block copolymers.

310

311

312

313

314

315

316

317

318

319

320

321

322

323

324

325

326

327

328

329

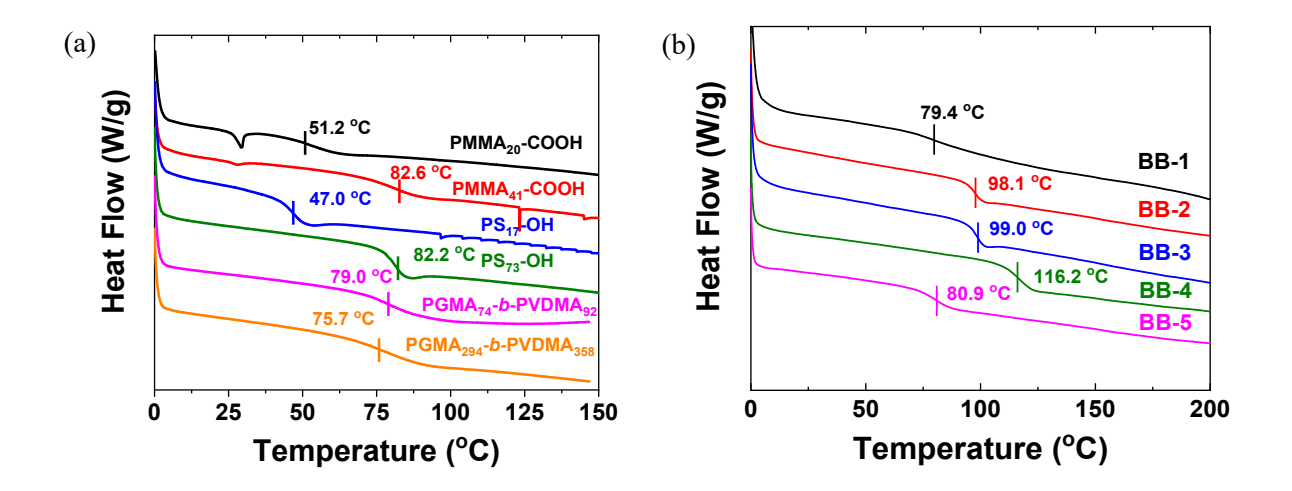


Figure 2. DSC analysis of (a) PGMA-*b*-PVDMA backbones and PS and PMMA grafts and (b) for BB-1 through BB-5.

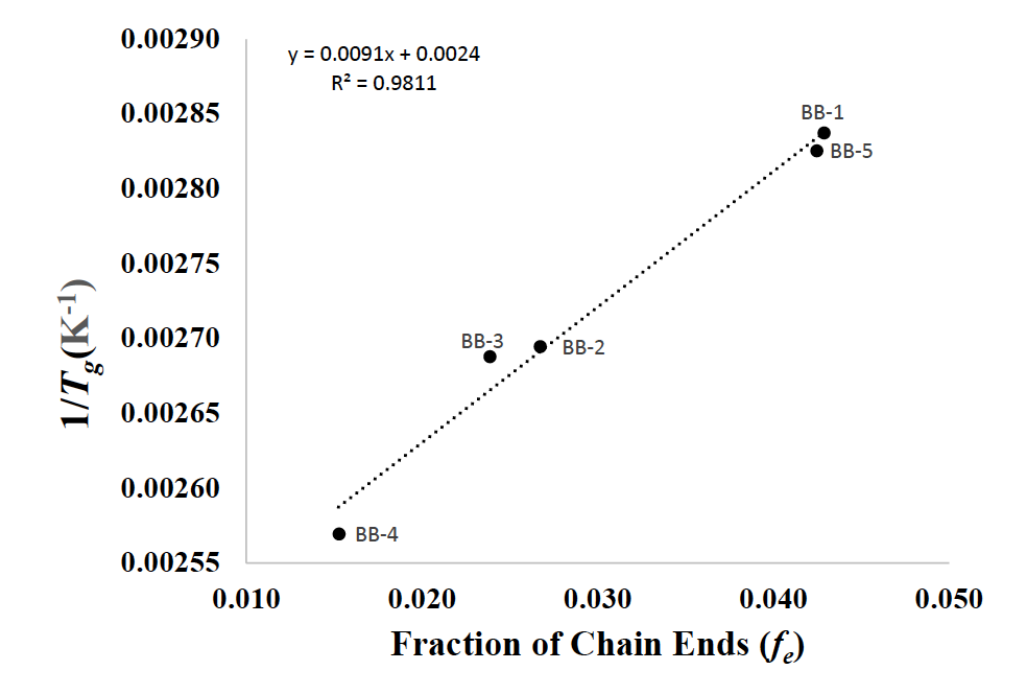


Figure 3. Self-plasticization due to chain ends in five bottlebrush block copolymer is shown by plotting $1/T_g$ (K⁻¹) as a function of the fraction of chain ends (f_e) (see **Table S4** for the estimations).

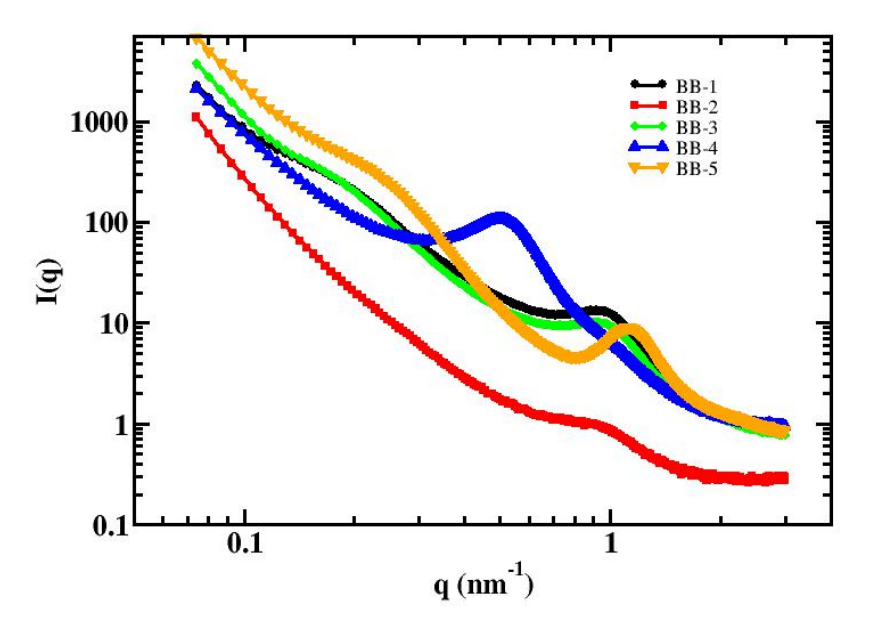


Figure 4. SAXS data collected on five bottlebrush samples at 130 °C showing at least one and sometimes two broad peaks (e.g., in the cases of BB-1,BB-3, and BB-5) hinting at segregation at two characteristic length scales.

Microphase separated bottlebrush block copolymers should exhibit multiple small-angle X-ray scattering (SAXS) peaks similar to linear diblock copolymers of PS and PMMA due to the periodic microdomain structure having a long-range order. 42-44 Information of the microphase morphology can be obtained from the relative positions of the SAXS peaks which are associated with the microdomain packing. For instance, the ratio of the q values at the scattering maxima are expected to be 1, 2, 3, 4,... for lamellae, 1, $\sqrt{3}$, $\sqrt{4}$, $\sqrt{7}$, $\sqrt{9}$... for cylinders in a hexagonal array, and 1, $\sqrt{2}$, $\sqrt{3}$, $\sqrt{4}$, $\sqrt{5}$,... for spheres in a body-centered cubic array. For example, Rzayev and coworkers reported a grafted-from bottlebrush system with a PMMA volume fraction of 41% and the SAXS

data showed a number higher order SAXS peaks that were consistent with a hexagonally packed morphology. 45 However, SAXS date for the bottlebrushes in the present study failed to produce higher order SAXS peaks (Figure 4) which indicate the absence of well-ordered microdomain packing. The SAXS intensity profiles do show strong primary SAXS peaks for each sample, that correspond to the interdomain distance, d, which increases from 6.5 to 12.2 nm with increasing graft molecular mass. Furthermore, secondary peaks are also observed in samples BB-1, BB-3, and BB-5. The morphology of the bottlebrush copolymers films was also investigated using AFM. All the samples were annealed at 130 °C for 24 h to assist the microphase separation between the two blocks. Figure 5 shows the observed AFM height images of BB-1 to BB-5. These images exhibit no signature of any long-range ordered morphology such as lamellae, hexagonally packed cylinders, etc. predicted by the SCFT (see Figure S2-S4). The AFM results were consistent with SAXS and point toward a disordered phase in the melts of the copolymers. To further confirm the absence of ordered morphology, small-amplitude oscillatory shear measurements were performed on BB-5 in the temperature range of 250—115°C. The dynamic moduli determined at different temperatures (Figure 6(a)) can be collapsed onto master curves by using either the Cole-Cole plot (Figure 6(b)) or time-temperature superposition (Figure 6(c)).⁵¹ Additionally, the obtained linear viscoelastic master curve (Figure 6(c)) resembles that of an entangled polymeric liquid, with a rubbery plateau at intermediate frequencies and terminal flow behavior at low frequencies. These results clearly indicate the absence of an order-disorder transition and the low-frequency liquidlike behavior suggests that the sample is in a disordered state.

351

352

353

354

355

356

357

358

359

360

361

362

363

364

365

366

367

368

369

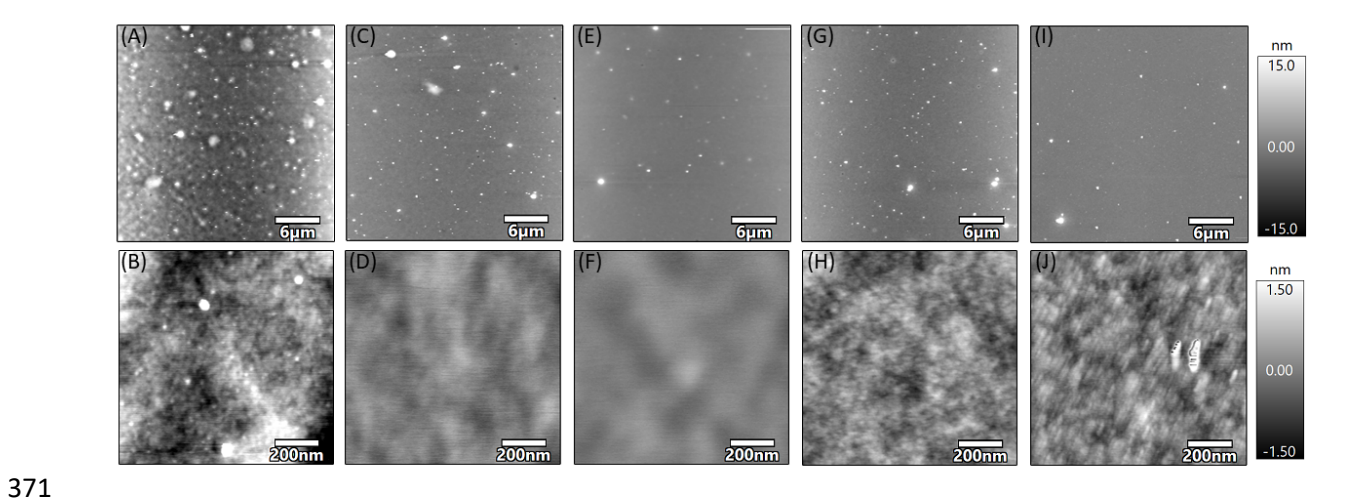


Figure 5. AFM topography images collected over a (A,C,E,G,I) 30 x 30 μm² and a smaller (B,D,F,H,J) 1 x 1 μm² -region. Data is shown for samples (A,B) BB-1, (C,D) BB-2, (E,F) BB-3, (G,H) BB-4, and (I,J) BB-5.

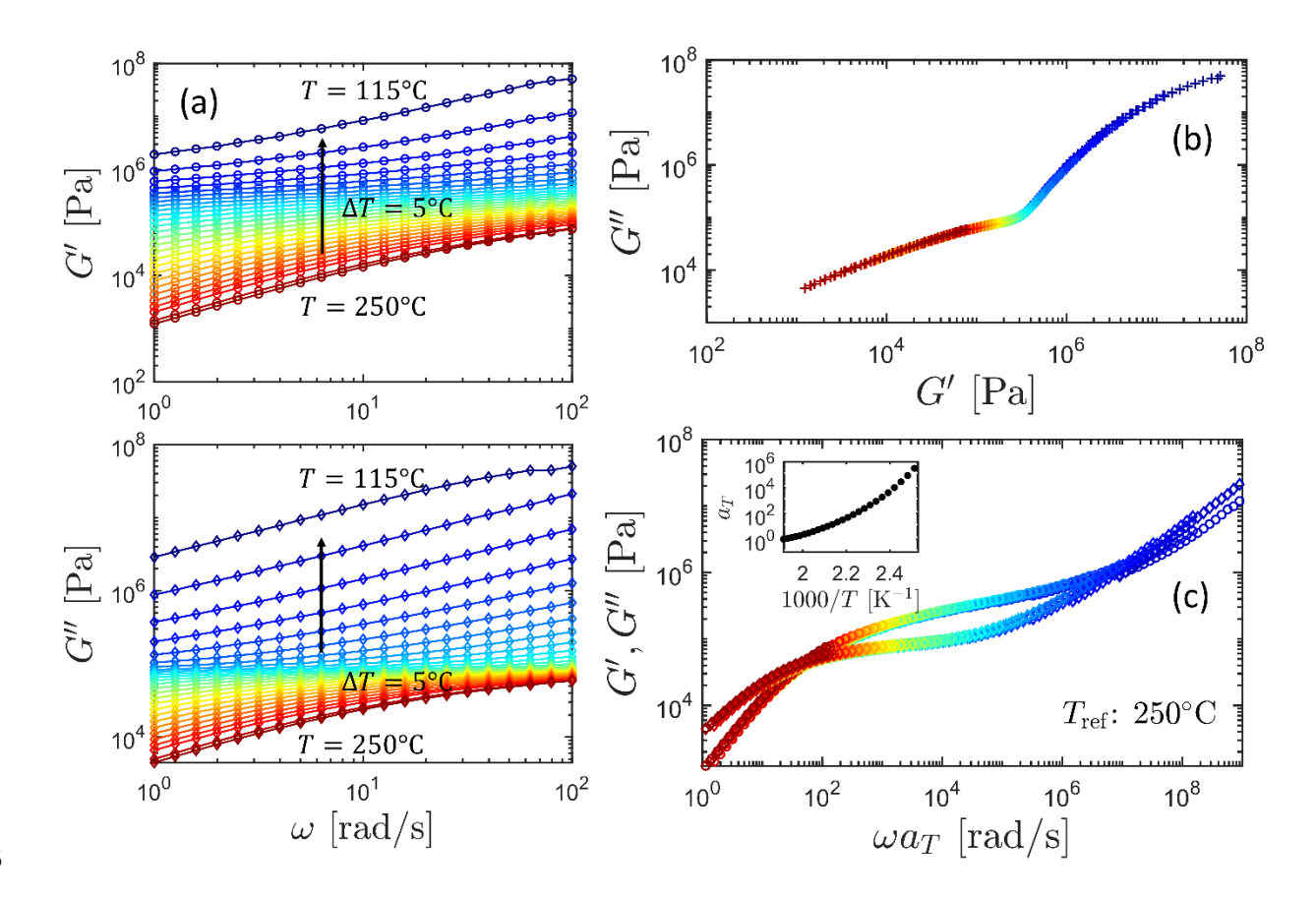
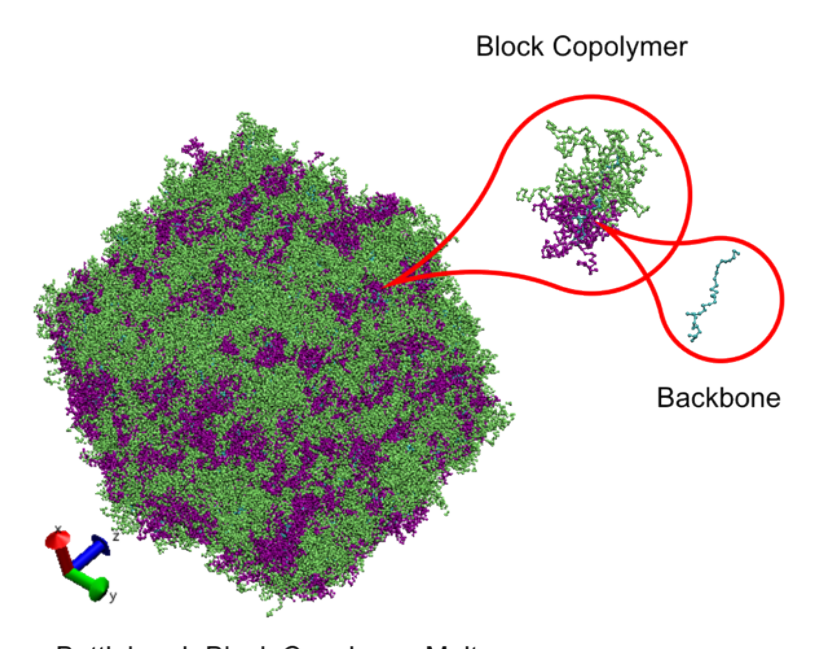


Figure 6. Linear viscoelastic properties of BB-5. (a) Storage $G'(\omega)$ and loss modulus $G''(\omega)$ of BB-5 at different temperatures. The results are color-coded with the "jet" colormap of MATLAB. The high-temperature data appear as reddish colors, whereas the low-temperature results are represented by bluish colors. (b) Cole-Cole plot of the data in (a), where the loss modulus is shown as a function of the storage modulus. (c) Master curve of dynamic moduli constructed according to the time-temperature superposition principle. The reference temperature is 250°C. Inset of (c): corresponding temperature shift factor a_T .



Bottlebrush Block Copolymer Melt

Figure 7. Snapshot of simulation box of a melt consisting of bottlebrush diblock copolymer. Beads belonging to A-block, B-block and backbone are colored magenta, green and cyan, respectively.

To understand the origin of the SAXS peaks despite the lack of ordering, we conducted coarsegrained MD simulations to compute the partial structure factors of disordered melts of bottlebrush

block copolymers. A similar analysis of the structure factor of bottlebrush melts was presented recently by Liang et al.⁵² A typical snapshot from the MD simulations of athermal melts of the copolymers is shown in Figure 7 with multi-scale structures in disordered melts of these copolymers. Furthermore, based on the electron density of PS, PMMA, PGMA, and PVDMA (=9.61, 10.84, 9.74, and 9.57 x 10^{-6} Å⁻², respectively), the partial structure factor, $S_{BB}(q)$, was chosen to understand the qualitative effects of graft lengths (at fixed grafting densities) on the SAXS spectra. By ignoring slight differences in the electron density values of PS, PGMA, and PVDMA, B was chosen to represent PMMA, enabling a qualitative comparison between the simulated spectra and the SAXS results. The partial structure factor spectra are shown in Figure 8(a) as the number of beads along a B-graft is varied from 5 to 80. The partial structure factor exhibits three peaks (e.g., for $N_B = 5$), where the peak at $q/\sigma \sim 7$ represents density-density correlations at the length scale of a single bead. The other two peaks represent correlations at larger length scales are comparable to the peaks observed in SAXS data. With an increase in N_B, the peak at intermediate wave-vector values disappears. The microscopic origin of the two length scales (larger than that of the monomer size) lies in the backbone-to-backbone and graft-to-graft correlations as shown in **Figure 8(b)**. Specifically, the peak at intermediate wave-vectors results from backbone-to-backbone correlations (S_{bb}), and an increase in N_B leads to a shift of the peak representing such correlations to lower wave-vectors. The peak at the lower wave-vectors represents lamellar-like organization of a bottlebrush chain and is independent of the graft length. This peak will shift with a change in either the backbone length or fraction of backbone monomers belonging to A. In fact, this is the reason that the primary peak in the SAXS for BB-5 is shifted in comparison with the other samples.

390

391

392

393

394

395

396

397

398

399

400

401

402

403

404

405

406

407

408

409

410

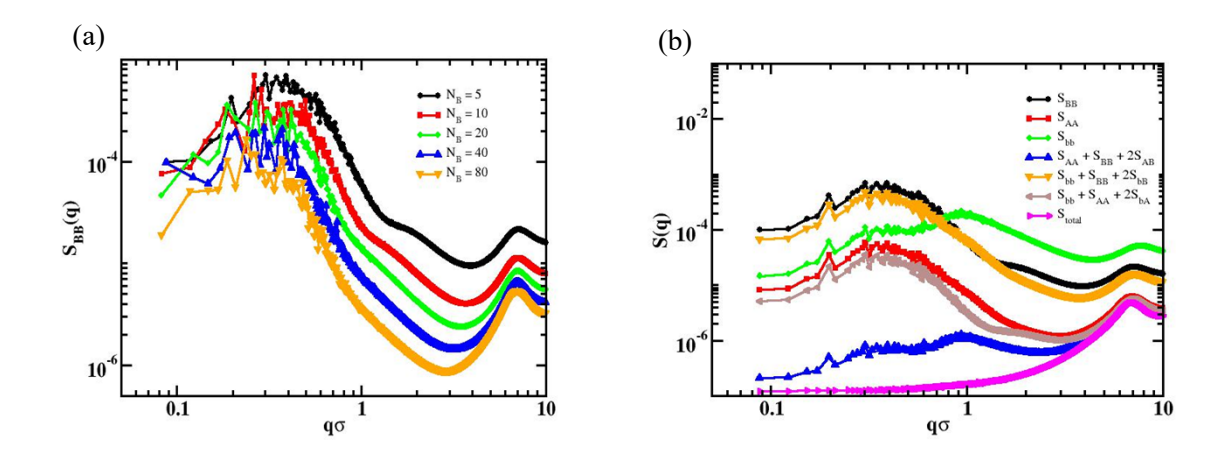


Figure 8. Generated SAXS plots from MD simulations: (a) effects of graft length on partial structure factor (S_{BB}) representative of SAXS experimental data shown in Figure 4(a). (b) All of the partial structure factors are shown for N_B = 5. Peaks at highest wave-vector results from finite-sized monomeric beads and the other two peaks represent two length scales related to graft lengths

and block lengths along the backbone separating A and B grafts.

Lastly, we used self-consistent field theory (SCFT) (see **Figures S2-S4** and **SI** for details) to study the disorder-order transition boundary for different ratios of side chain lengths as a function of the relative ratio of side chain segments, $f_M/(f_S + f_M)$. These results are shown in **Figure 9**. Here, $f_i = N_i/N$ is simply the overall fraction of segments in each bottlebrush block copolymer of type i, and "S" and "M" denote the two types of grafts. It is notable that the value of χN required to manifest the transition from a disordered state to an ordered state is significantly higher ($\chi_{SM}N \approx 30$) compared to linear diblock copolymers ($\chi N \approx 10$). These results imply that the bottlebrush block chain architecture stabilizes the disordered phase over ordered morphologies and provide justification for the observation of a disordered morphology in all five bottlebrushes.

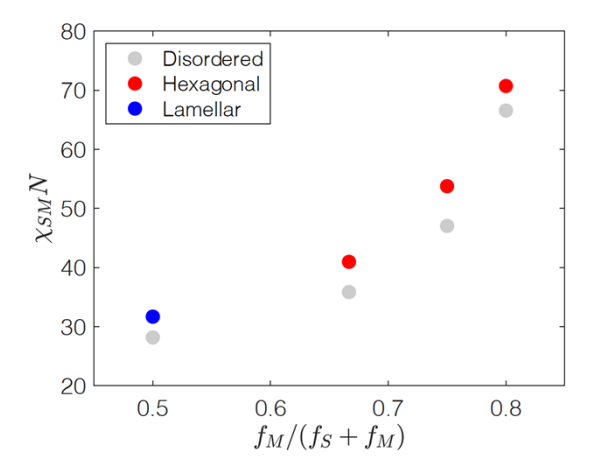


Figure 9: Disorder-order transition boundary estimated in terms of interaction parameter χ_{SM} (representing interaction among unlike grafts) as a function of relative ratio of side chain segments for $\chi_{ME} = \chi_{SE} = 0$.

Conclusions

A 'toolbox' that enables the synthesis of bottlebrush AB diblock copolymers was developed by grafting -OH and -COOH end functionalized polymers onto PGMA-b-PVDMA backbones via a two-step reaction that leverages preferential reactivity of the backbone epoxide and azlactone groups. Five PGMA(-g-PMMA)-b-PVDMA(-g-PS) bottlebrush block copolymers were synthesized and characterized by SEC, ¹H NMR, and FT-IR. The thermal properties, as well as the morphology of the bottlebrush diblock copolymers, were investigated by DSC, SAXS, AFM and rheology. The chain ends act as self-plasticizers in the bottlebrush block copolymers and the *fraction of chain ends* was found to affect the glass transition temperature of bottlebrush block copolymers. Although the samples were found to be in the disordered phase, SAXS indicated that multi-scale structures were present, which can be attributed to graft-to-graft and backbone-to-backbone density correlations as revealed by MD simulations. Furthermore, SCFT simulations indicate that the grafts serve as stabilizers for the disordered morphology and as a result, ordered

phases were not observed in this work. The synthetic strategy presented here represents a platform to graft a variety of polymer side chains onto a backbone. This modular approach can be easily extended to other grafts, including functional polymers, with the prerequisite end groups making this a versatile method for the synthesis of novel bottlebrush block copolymers with desired properties. This will be the subject of our future research efforts.

Supporting Information

Experimental details for reactivity test and results (Table S1). SEC analysis of diblock copolymer and grafts (Figure S1). Molecular weights and bottle brush grafting description and results (Table S2 and Equations 1-11). Glass transition temperatures of the grafts and the parent block copolymers (Table S3). Diblock bottle brush glass transition temperatures, number repeat units for the backbone and total grafts, number of chain ends, and fraction of chain ends to total repeat units (Table S4). Experimental details for coarse-grained molecular dynamics simulations. Experimental details for self-consistent field theory simulations, schematic of structure, simulated morphologies, and partial structure factors versus graft lengths (Figure S2-S4).

Acknowledgement

This research was conducted at the Center for Nanophase Materials Sciences, Oak Ridge National Laboratory which is a U.S. Department of Energy, Office of Science User Facility. Oak Ridge National Laboratory is operated for DOE Office of Science by UT Battelle, LLC, under contract number DE-AC05-00OR22725. K.S.S was supported by the Department of Energy Computational Science Graduate Fellowship program under grant DE-FG02-97ER25308.

References

- 1. Sheiko, S. S.; Sumerlin, B. S.; Matyjaszewski, K., Cylindrical molecular brushes:
- Synthesis, characterization, and properties. *Progress in Polymer Science* **2008**, *33* (7), 759-785.
- 469 2. Xia, Y.; Olsen, B. D.; Kornfield, J. A.; Grubbs, R. H., Efficient synthesis of narrowly
- 470 dispersed brush copolymers and study of their assemblies: the importance of side chain
- 471 arrangement. J Am Chem Soc **2009**, 131 (51), 18525-32.
- 472 3. Zhang, M.; Müller, A. H. E., Cylindrical polymer brushes. *Journal of Polymer Science*
- 473 *Part A: Polymer Chemistry* **2005,** *43* (16), 3461-3481.
- 474 4. Bolton, J.; Rzayev, J., Synthesis and Melt Self-Assembly of PS-PMMA-PLA Triblock
- 475 Bottlebrush Copolymers. *Macromolecules* **2014**, *47* (9), 2864-2874.
- 476 5. Verduzco, R.; Li, X.; Pesek, S. L.; Stein, G. E., Structure, function, self-assembly, and
- applications of bottlebrush copolymers. *Chem Soc Rev* **2015**, *44* (8), 2405-20.
- 478 6. Cai, L. H.; Kodger, T. E.; Guerra, R. E.; Pegoraro, A. F.; Rubinstein, M.; Weitz, D. A.,
- 479 Soft Poly(dimethylsiloxane) Elastomers from Architecture-Driven Entanglement Free Design.
- 480 *Adv Mater* **2015,** *27* (35), 5132-40.
- 481 7. Mah, A. H.; Afzali, P.; Qi, L.; Pesek, S.; Verduzco, R.; Stein, G. E., Bottlebrush Copolymer
- Additives for Immiscible Polymer Blends. *Macromolecules* **2018**, *51* (15), 5665-5675.
- 483 8. Mei, H.; Laws, T. S.; Mahalik, J. P.; Li, J.; Mah, A. H.; Terlier, T.; Bonnesen, P.; Uhrig,
- D.; Kumar, R.; Stein, G. E.; Verduzco, R., Entropy and Enthalpy Mediated Segregation of
- Bottlebrush Copolymers to Interfaces. *Macromolecules* **2019**, *52* (22), 8910-8922.
- Johnson, J. A.; Lu, Y. Y.; Burts, A. O.; Xia, Y.; Durrell, A. C.; Tirrell, D. A.; Grubbs, R.
- 487 H., Drug-loaded, bivalent-bottle-brush polymers by graft-through ROMP. *Macromolecules* **2010**,
- 488 *43* (24), 10326-10335.

- 489 10. Foster, J. C.; Varlas, S.; Couturaud, B.; Coe, Z.; O'Reilly, R. K., Getting into Shape:
- 490 Reflections on a New Generation of Cylindrical Nanostructures' Self-Assembly Using Polymer
- 491 Building Blocks. J Am Chem Soc **2019**, 141 (7), 2742-2753.
- 492 11. Kent, E. W.; Henn, D. M.; Zhao, B., Shape-changing linear molecular bottlebrushes with
- 493 dually pH- and thermo-responsive diblock copolymer side chains. *Polymer Chemistry* **2018**, 9 (41),
- 494 5133-5144.
- 495 12. Li, X.; Prukop, S. L.; Biswal, S. L.; Verduzco, R., Surface Properties of Bottlebrush
- 496 Polymer Thin Films. *Macromolecules* **2012**, *45* (17), 7118-7127.
- 497 13. Liberman-Martin, A. L.; Chu, C. K.; Grubbs, R. H., Application of Bottlebrush Block
- 498 Copolymers as Photonic Crystals. *Macromol Rapid Commun* **2017**, *38* (13), 1700058.
- 499 14. Henn, D. M.; Fu, W.; Mei, S.; Li, C. Y.; Zhao, B., Temperature-Induced Shape Changing
- of Thermosensitive Binary Heterografted Linear Molecular Brushes between Extended Wormlike
- and Stable Globular Conformations. *Macromolecules* **2017**, *50* (4), 1645-1656.
- 502 15. Fenyves, R.; Schmutz, M.; Horner, I. J.; Bright, F. V.; Rzayev, J., Aqueous self-assembly
- of giant bottlebrush block copolymer surfactants as shape-tunable building blocks. *J Am Chem Soc*
- **2014,** *136* (21), 7762-70.
- 505 16. Dalsin, S. J.; Hillmyer, M. A.; Bates, F. S., Linear Rheology of Polyolefin-Based
- 506 Bottlebrush Polymers. *Macromolecules* **2015**, *48* (13), 4680-4691.
- 507 17. Alaboalirat, M.; Qi, L.; Arrington, K. J.; Qian, S.; Keum, J. K.; Mei, H.; Littrell, K. C.;
- Sumpter, B. G.; Carrillo, J.-M. Y.; Verduzco, R.; Matson, J. B., Amphiphilic Bottlebrush Block
- 509 Copolymers: Analysis of Aqueous Self-Assembly by Small-Angle Neutron Scattering and Surface
- Tension Measurements. *Macromolecules* **2018**, *52* (2), 465-476.

- 511 18. Walsh, D. J.; Wade, M. A.; Rogers, S. A.; Guironnet, D., Challenges of Size-Exclusion
- 512 Chromatography for the Analysis of Bottlebrush Polymers. *Macromolecules* **2020**, *53* (19), 8610-
- 513 8620.
- 514 19. Gao, H.; Matyjaszewski, K., Synthesis of molecular brushes by "grafting onto" method:
- combination of ATRP and click reactions. J Am Chem Soc 2007, 129 (20), 6633-9.
- 516 20. Rzayev, J., Synthesis of Polystyrene–Polylactide Bottlebrush Block Copolymers and Their
- Melt Self-Assembly into Large Domain Nanostructures. *Macromolecules* **2009**, *42* (6), 2135-2141.
- 518 21. Miyake, G. M.; Piunova, V. A.; Weitekamp, R. A.; Grubbs, R. H., Precisely tunable
- 519 photonic crystals from rapidly self-assembling brush block copolymer blends. *Angew Chem Int Ed*
- 520 Engl **2012**, 51 (45), 11246-8.
- 521 22. Hillmyer, M. A.; Lepetit, C.; McGrath, D. V.; Novak, B. M.; Grubbs, R. H., Aqueous ring-
- 522 opening metathesis polymerization of carboximide-functionalized 7-oxanorbornenes.
- 523 *Macromolecules* **2002,** *25* (13), 3345-3350.
- 524 23. Henn, D. M.; Lau, C. M.; Li, C. Y.; Zhao, B., Light-triggered unfolding of single linear
- 525 molecular bottlebrushes from compact globular to wormlike nano-objects in water. Polymer
- 526 *Chemistry* **2017**, 8 (17), 2702-2712.
- 527 24. Tang, H.; Li, Y.; Lahasky, S. H.; Sheiko, S. S.; Zhang, D., Core-Shell Molecular
- 528 Bottlebrushes with Helical Polypeptide Backbone: Synthesis, Characterization, and Solution
- 529 Conformations. *Macromolecules* **2011**, *44* (6), 1491-1499.
- 530 25. Shahrokhinia, A.; Biswas, P.; Reuther, J. F., Orthogonal synthesis and modification of
- 531 polymer materials. *Journal of Polymer Science* **2021**, *59* (16), 1748-1786.
- 532 26. Corrigan, N.; Ciftci, M.; Jung, K.; Boyer, C., Mediating Reaction Orthogonality in Polymer
- and Materials Science. *Angew Chem Int Ed Engl* **2021**, *60* (4), 1748-1781.

- 534 27. Han, D.; Tong, X.; Zhao, Y., One-pot synthesis of brush diblock copolymers through
- simultaneous ATRP and click coupling. *Macromolecules* **2011**, *44* (13), 5531-5536.
- 536 28. Bolton, J.; Rzayev, J., Tandem RAFT-ATRP Synthesis of Polystyrene-Poly(Methyl
- 537 Methacrylate) Bottlebrush Block Copolymers and Their Self-Assembly into Cylindrical
- 538 Nanostructures. *ACS Macro Letters* **2011**, *1* (1), 15-18.
- 539 29. Lokitz, B. S.; Wei, J.; Hinestrosa, J. P.; Ivanov, I.; Browning, J. F.; Ankner, J. F.; Kilbey,
- 540 S. M.; Messman, J. M., Manipulating Interfaces through Surface Confinement of Poly(glycidyl
- 541 methacrylate)-block-poly(vinyldimethylazlactone), a Dually Reactive Block Copolymer.
- 542 *Macromolecules* **2012,** *45* (16), 6438-6449.
- 543 30. Hansen, R. R.; Hinestrosa, J. P.; Shubert, K. R.; Morrell-Falvey, J. L.; Pelletier, D. A.;
- Messman, J. M.; Kilbey, S. M., 2nd; Lokitz, B. S.; Retterer, S. T., Lectin-functionalized
- 545 poly(glycidyl methacrylate)-block-poly(vinyldimethyl azlactone) surface scaffolds for high
- avidity microbial capture. *Biomacromolecules* **2013**, *14* (10), 3742-8.
- 547 31. Barkakaty, B.; Browning, K. L.; Sumpter, B.; Uhrig, D.; Karpisova, I.; Harman, K. W.;
- Ivanov, I.; Hensley, D. K.; Messman, J. M.; Kilbey, S. M.; Lokitz, B. S., Amidine-Functionalized
- Poly(2-vinyl-4,4-dimethylazlactone) for Selective and Efficient CO2 Fixing. Macromolecules
- **2016,** *49* (5), 1523-1531.
- 32. Aden, B.; Kite, C. M.; Hopkins, B. W.; Zetterberg, A.; Lokitz, B. S.; Ankner, J. F.; Kilbey,
- 552 S. M., Assessing Chemical Transformation of Reactive, Interfacial Thin Films Made of End-
- Tethered Poly(2-vinyl-4,4-dimethyl azlactone) (PVDMA) Chains. *Macromolecules* **2017**, *50* (2),
- 554 618-630.

- 555 33. Masigol, M.; Fattahi, N.; Barua, N.; Lokitz, B. S.; Retterer, S. T.; Platt, T. G.; Hansen, R.
- R., Identification of Critical Surface Parameters Driving Lectin-Mediated Capture of Bacteria from
- 557 Solution. *Biomacromolecules* **2019**, *20* (7), 2852-2863.
- 558 34. Muzammil, Ezzah M.; Khan, A.; Stuparu, M. C., Post-polymerization modification
- reactions of poly(glycidyl methacrylate)s. RSC Advances 2017, 7 (88), 55874-55884.
- 560 35. Zhu, Y.; Quek, J. Y.; Lowe, A. B.; Roth, P. J., Thermoresponsive (Co)polymers through
- Postpolymerization Modification of Poly(2-vinyl-4,4-dimethylazlactone). *Macromolecules* **2013**,
- 562 *46* (16), 6475-6484.
- 563 36. Plimpton, S., Fast Parallel Algorithms for Short-Range Molecular Dynamics. Journal of
- 564 *Computational Physics* **1995,** *117* (1), 1-19.
- 565 37. Brown, W. M.; Wang, P.; Plimpton, S. J.; Tharrington, A. N., Implementing molecular
- 566 dynamics on hybrid high performance computers short range forces. Computer Physics
- 567 *Communications* **2011**, *182* (4), 898-911.
- 568 38. Carrillo, J.-M. Y.; Dobrynin, A. V., Polyelectrolytes in Salt Solutions: Molecular
- 569 Dynamics Simulations. *Macromolecules* **2011**, *44* (14), 5798-5816.
- 570 39. Sides, S. W.; Fredrickson, G. H., Parallel algorithm for numerical self-consistent field
- 571 theory simulations of block copolymer structure. *Polymer* **2003**, *44* (19), 5859-5866.
- Heilmann, S. M.; Moren, D. M.; Krepski, L. R.; Pathre, S. V.; Rasmussen, J. K.; Stevens,
- J., The chemistry of 2-alkenyl-5 (4H)-oxazolones. VIII acid-catalyzed reaction with alcohols.
- 574 *Tetrahedron* **1998**, *54* (40), 12151-12160.
- 575 41. Kudo, H.; Buya, K., Mechanistic study of ring-opening copolymerization of ε-caprolactam
- 576 with epoxide: Development of novel thermosetting epoxy resin system. Journal of Polymer
- 577 *Science Part A: Polymer Chemistry* **2016,** *54* (14), 2220-2228.

- 578 42. Ahn, H.; Ryu, D. Y.; Kim, Y.; Kwon, K. W.; Lee, J.; Cho, J., Phase Behavior of
- Polystyrene-b-poly(methyl methacrylate) Diblock Copolymer. *Macromolecules* **2009**, *42* (20),
- 580 7897-7902.
- 581 43. Seo, Y. S.; Kim, E.; Kwon, S. Y.; Jing, H.; Shin, K., AFM study of phase-separated
- morphology in immiscible blend thin films. *Ultramicroscopy* **2008**, *108* (10), 1186-90.
- 583 44. Guo, R.; Kim, E.; Gong, J.; Choi, S.; Ham, S.; Ryu, D. Y., Perpendicular orientation of
- microdomains in PS-b-PMMA thin films on the PS brushed substrates. Soft Matter 2011, 7 (15),
- 585 6920.
- 586 45. Mah, A. H.; Laws, T.; Li, W.; Mei, H.; Brown, C. C.; Ievley, A.; Kumar, R.; Verduzco, R.;
- 587 Stein, G. E., Entropic and Enthalpic Effects in Thin Film Blends of Homopolymers and
- 588 Bottlebrush Polymers. *Macromolecules* **2019**, *52* (4), 1526-1535.
- 589 46. Ueberreiter, K.; Kanig, G., Self-plasticization of polymers. Journal of Colloid Science
- **1952,** *7* (6), 569-583.
- 591 47. Bocharova, V.; Wojnarowska, Z.; Cao, P. F.; Fu, Y.; Kumar, R.; Li, B.; Novikov, V. N.;
- Zhao, S.; Kisliuk, A.; Saito, T.; Mays, J. W.; Sumpter, B. G.; Sokolov, A. P., Influence of Chain
- 593 Rigidity and Dielectric Constant on the Glass Transition Temperature in Polymerized Ionic
- 594 Liquids. *J Phys Chem B* **2017**, *121* (51), 11511-11519.
- 595 48. Zhang, L.; Torkelson, J. M., Enhanced glass transition temperature of low molecular
- weight poly(methyl methacrylate) by initiator fragments located at chain ends. *Polymer* **2017**, *122*,
- 597 194-199.
- 598 49. Santangelo, P. G.; Roland, C. M., Molecular Weight Dependence of Fragility in
- 599 Polystyrene. *Macromolecules* **1998,** *31* (14), 4581-4585.

- 600 50. Chu, B.; Hsiao, B. S., Small-angle X-ray scattering of polymers. Chem Rev 2001, 101 (6),
- 601 1727-61.
- 602 51. Ferry, J. D., Viscoelastic properties of polymers. John Wiley & Sons: 1980.
- 603 52. Liang, H.; Wang, Z.; Dobrynin, A. V., Scattering from Melts of Combs and Bottlebrushes:
- Molecular Dynamics Simulations and Theoretical Study. Macromolecules 2019, 52 (15), 5555-
- 605 5562.